nature structural & molecular biology

miRNA-mediated deadenylation is orchestrated by GW182 through two conserved motifs that interact with CCR4–NOT

Marc R Fabian[1,2], Maja K Cieplak[3], Filipp Frank[1,2], Masahiro Morita[1,2,4], Jonathan Green[1,2], Tharan Srikumar[5], Bhushan Nagar[1,2], Tadashi Yamamoto[4], Brian Raught[5], Thomas F Duchaine[1,2] & Nahum Sonenberg[1,2]

miRNAs recruit the miRNA-induced silencing complex (miRISC), which includes Argonaute and GW182 as core proteins. GW182 proteins effect translational repression and deadenylation of target mRNAs. However, the molecular mechanisms of GW182-mediated repression remain obscure. We show here that human GW182 independently interacts with the PAN2–PAN3 and CCR4–NOT deadenylase complexes. Interaction of GW182 with CCR4–NOT is mediated by two newly discovered phylogenetically conserved motifs. Although either motif is sufficient to bind CCR4–NOT, only one of them can promote processive deadenylation of target mRNAs. Thus, GW182 serves as both a platform that recruits deadenylases and as a deadenylase coactivator that facilitates the removal of the poly(A) tail by CCR4–NOT.

MicroRNAs (miRNAs) are short (~22 nucleotide (nt)) noncoding RNAs that silence target mRNAs at the post-transcriptional level[1–3]. In general, miRNAs repress protein synthesis by imperfectly base pairing to the 3′ UTRs of target mRNAs and inhibit translation and/or initiate mRNA deadenylation and decay[1–3]. miRNAs recruit a protein complex called the miRNA-induced silencing complex (miRISC). The miRISC core consists of a miRNA-loaded Argonaute protein (AGO) and the AGO-interacting GW182 protein.

Animal AGO proteins are essential for miRNA-mediated repression of target mRNAs but on their own are, in general, insufficient for silencing. Depleting GW182 proteins from mammalian and insect cells abrogates miRNA silencing[4–9]. Moreover, artificially tethering GW182 proteins to targeted mRNAs in the absence of AGO proteins engenders robust repression[6,10–15]. Thus, GW182 proteins are important miRISC effectors, and AGO proteins in the most general case function to recruit GW182 proteins to miRNA-targeted mRNAs. However, it is unclear how GW182 proteins bring about miRNA-mediated gene silencing.

Insects encode a single GW182 protein, called Gawky, whereas mammals encode three GW182 paralogs (TNRC6A, TNRC6B and TNRC6C)[16]. GW182 proteins directly bind AGOs through several glycine-tryptophan (GW) repeats in their N termini (**Fig. 1a**)[4,17,18]. GW182 proteins contain additional domains including two globular domains: a ubiquitin-associated (UBA) domain and a noncanonical RNA recognition motif (RRM) that appears not to bind RNA (**Fig. 1a**)[19]. Although the GW182 N terminus is important for binding AGO, it is the C-terminal region of GW182 proteins, termed the 'silencing domain' (**Fig. 1a**), that is responsible for robust silencing[10,12,13,15,20,21]. The silencing domain is a bipartite region, which is predicted to be unstructured. It is divided into middle (Mid) and C-terminal (C-term) subdomains that flank the RRM (**Fig. 1b**). The Mid domain is further subdivided into the M1 and M2 regions that flank a PABP-interacting (PAM2) motif[15,22,23].

Mammals encode two major enzyme complexes that are responsible for mRNA deadenylation: the multisubunit CCR4–NOT complex and the heterodimeric PAN2–PAN3 complex[24]. We previously reported that in addition to PABP, the mammalian miRISC associates with the CAF1 (CNOT7) and CCR4b (CNOT6L) deadenylases, the 3′–5′ exonuclease subunits of the CCR4–NOT complex, suggesting a model whereby the miRISC recruits the deadenylase machinery to target mRNAs[15,23].

We show here that human GW182 interacts with the CCR4–NOT deadenylase complex through two newly discovered phylogenetically conserved motifs to effect miRNA-mediated deadenylation. The motifs reside at the opposite ends of the GW182 silencing domain; one within the M1 region of the Mid domain and the other within the C-terminal domain. We demonstrate that the CCR4–NOT deadenylase complex interacts directly—and independently of PABP—with GW182 through the CNOT1 subunit. In addition, GW182 recruits the PAN2–PAN3 deadenylase complex through the PAM2 motif. Thus, the GW182 silencing domain serves as a platform that assembles a large complex that includes PABP and the deadenylation machineries. Furthermore, we show that GW182 also functions as a deadenylation coactivator by aiding the CCR4–NOT complex to remove the poly(A) tail.

[1]Department of Biochemistry, McGill University, Montreal, Canada. [2]Goodman Cancer Centre, McGill University, Montreal, Canada. [3]Department of Biophysics, Institute of Experimental Physics, Warsaw University, Warsaw, Poland. [4]Department of Cancer Biology, Institute of Medical Science, University of Tokyo, Tokyo, Japan. [5]Ontario Cancer Institute, University of Toronto, Toronto, Canada. Correspondence should be addressed to N.S. (nahum.sonenberg@mcgill.ca).

Received 6 July; accepted 31 August; published online 7 October 2011; doi:10.1038/nsmb.2149

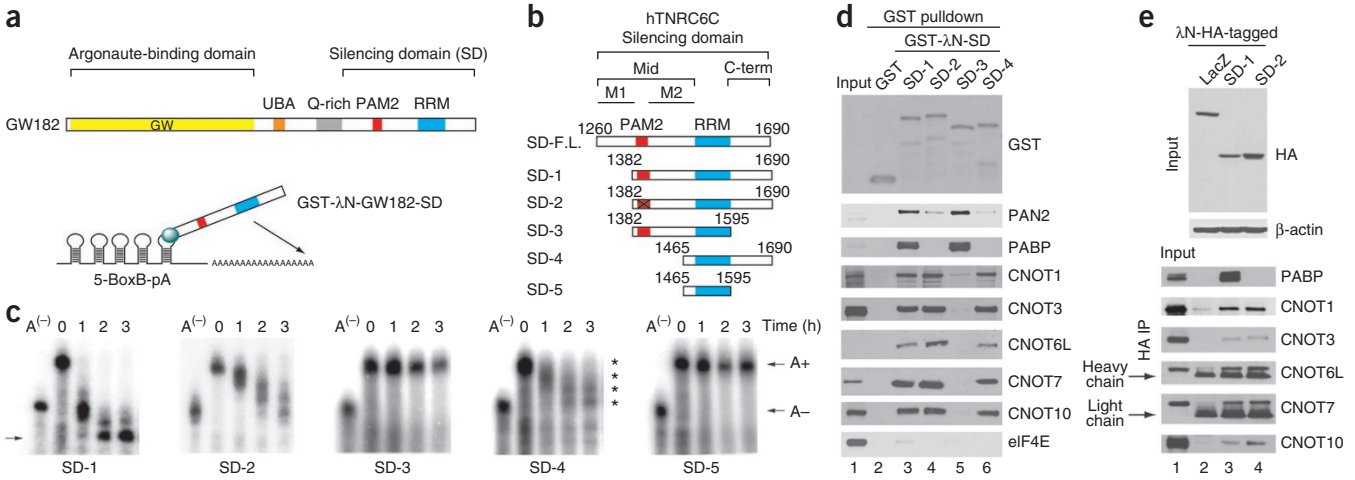

Figure 1 Mammalian GW182 protein silencing domain (SD) interacts with PABP and the CCR4–NOT deadenylase complex through independent domains to promote deadenylation. (**a**) Schematic diagrams of the human GW182 protein and *in vitro* deadenylation assays in Krebs extract. Human GW182 paralogs (TNRC6A, TNRC6B and TNRC6C) have similar domain architecture. The glycine-tryptophan (GW), ubiquitin-associated (UBA), glutamine-rich (Q-rich) and silencing domain regions are indicated. Human (h)TNRC6C silencing domain fragments fused to the λN-peptide were tethered to a polyadenylated RNA containing five BoxB hairpins (5-BoxB-pA) in Krebs extracts. (**b**) Schematic representation of TNRC6C full-length silencing domain (SD-F.L.) and silencing domain fragments used in Krebs extract (**c**). (**c**) 5-BoxB-pA RNA deadenylation in the Krebs extract in the presence of GST-λN-HA-tagged TNRC6C fragments. Point mutations in GST-λN-HA-TNRC6C SD-2 have been previously described (a fragment previously termed $1382–1690_{PAM2\ MUT}$; see ref. 15). $A^{(-)}$ RNA was prepared by incubating 5-BoxB-pA with Oligo(dT) and RNase H. Polyadenylated and deadenylated mRNAs are marked on the right of the figure. RNAs shortened beyond the poly(A) tail are marked with an arrow on the left of the figure. Deadenylation intermediates for SD-4 are marked with asterisks. (**d**) Results from recombinant GST-λN-HA-tagged TNRC6C silencing domain fragments (**b**) that were immobilized on glutathione-Sepharose beads and incubated with RNase A–treated HeLa cell lysates. Precipitated proteins were separated by SDS-PAGE and probed with antibodies against the indicated proteins. (**e**) Immunoprecipitation (IP) of transiently transfected λN-HA-tagged proteins from RNase A–treated HeLa cell extracts using anti-HA antibody. Immunoprecipitated complexes were treated with SDS-PAGE and probed with antibodies against the indicated proteins.

RESULTS

GW182 C-terminal domain mediates deadenylation of target RNAs

We previously described a mammalian cell-free extract derived from mouse Krebs-2 ascites cells (referred throughout as Krebs extract) that recapitulates both miRNA-mediated translational repression and subsequent deadenylation of let-7 target mRNAs[23,25]. A GW182 silencing domain fragment (SD-1 (TNRC6C, coordinates 1382–1690)) caused deadenylation in a Krebs extract, as expected (**Fig. 1c**)[15]. Tethering SD-1 with a lambda N bacteriophage peptide (λN) to a polyadenylated RNA containing BoxB stem-loops (5-BoxB-pA), which mimics GW182 recruitment to a target RNA by AGO proteins, brought about poly(A) tail removal after 1 h incubation. Deadenylated RNA was further shortened (marked by an arrow to the left of the figure) after longer incubation and was terminated at the base of the last BoxB stem-loop (data not shown). miRNA-mediated deadenylation in *Caenorhabditis elegans* embryonic extract has shown a similar pattern of degradation kinetics[26]. Deadenylated RNAs remained relatively stable, providing a unique opportunity to investigate GW182-mediated deadenylation in the absence of RNA decay. Disrupting PABP binding to GW182 by mutating evolutionarily conserved residues to alanines in the PAM2 motif (Glu1388–Phe1389 and Trp1395–Lys1396; SD-2) reduced the rate, but not the extent, of deadenylation (**Fig. 1c**, compare SD-2 to SD-1; see also ref. 15), suggesting that additional sequences in the GW182 silencing domain contribute to miRNA-mediated deadenylation. To identify these sequences, we generated truncated silencing domain fragments (**Fig. 1b**), which were examined in deadenylation of 5-BoxB-pA RNA. A silencing domain fragment lacking the C-terminal domain (SD-3) failed to deadenylate 5-BoxB-pA RNA even after 3 h of incubation (**Fig. 1c**). In marked contrast to this, a fragment lacking the Mid domain (SD-4) promoted deadenylation when tethered to 5-BoxB-pA RNA, albeit with substantially attenuated rate and processivity as compared to SD-1 (**Fig. 1c**). Several intermediate products were observed (marked by asterisks). The RRM alone (SD-5) also failed to cause deadenylation. Thus, the GW182 C-terminal domain (TNRC6C coordinates 1596–1690) is essential for deadenylation of target RNAs. Moreover, our data demonstrate that the GW182 PAM2 motif that binds PABP is on its own insufficient to cause deadenylation of target RNAs.

GW182 interacts with CCR4–NOT and PAN2 by distinct motifs

Mammalian AGO proteins associate with the CAF1/CNOT7 and CCR4b/CNOT6L deadenylases[23]. Because the GW182 silencing domain promotes robust deadenylation when artificially tethered to a reporter RNA in the *in vitro* system (**Fig. 1c**)[15], it was pertinent to investigate whether it interacts with the deadenylation machinery. To this end, a glutathione-*S*-transferase (GST)-λN-hemagglutinin (HA)-tagged GW182 silencing domain fragment, which effects deadenylation (SD-1), was incubated in a HeLa cell extract that was treated with RNase A to ensure that protein-protein interactions were not mediated by RNA. Interacting proteins were separated by SDS-PAGE and identified by western blotting with antibodies against deadenylase subunits. SD-1 bound PABP, the PAN2 deadenylase and multiple components of the CCR4–NOT deadenylase complex (CNOT1, CNOT3, CCR4b/CNOT6L, CAF1/CNOT7 and CNOT10), but not the cap-binding translation initiation factor, eIF4E (**Fig. 1d**, lane 3). A silencing domain fragment with a mutant PAM2 motif (SD-2) failed to interact with PABP, as expected, and the bulk of the PAN2 deadenylase interaction was also lost (**Fig. 1d**, lane 4). The latter finding was not unexpected, as the PAN3 subunit of the PAN2–PAN3 complex directly binds PABP[27–29]. This markedly contrasts with SD-2

binding to the CCR4–NOT complex, which was not affected by the loss of PABP or PAN2 interaction with GW182 (**Fig. 1d**, compare lane 3 to 4). Similar results were observed in GST pulldowns with SD-1 and SD-2 from Krebs extract (**Supplementary Fig. 1**). The GW182-CCR4–NOT interaction was confirmed in cell cultures. Plasmids encoding the λN-HA-tagged SD-1 and SD-2 fragments were transiently transfected into HeLa cells, and the fragments were immunoprecipitated from RNase A–treated lysates with anti-HA antibody. Co-immunoprecipitating proteins were analyzed by western blotting (**Fig. 1e**). Similar amounts of CCR4–NOT deadenylase components (CNOT1, CNOT3, CNOT6L, CNOT7 and CNOT10) were bound with SD-1 and SD-2, whereas only SD-1 was bound to PABP (compare lane 3 to 4). λN-HA-LacZ, which served as a negative control, failed to associate with any of the proteins (lane 2). Thus, the data demonstrate that both the CCR4–NOT deadenylase complex and the PAN2 deadenylase interact with the silencing domain of human GW182 proteins. However, the PAN2 deadenylase and the CCR4–NOT complex are recruited to GW182 as separate protein complexes and through distinct motifs. The GW182 PAM2 motif assembles the PAN2 deadenylase, most likely through its interaction with PABP. By contrast, the GW182 silencing domain interacts with the CCR4–NOT complex in a PABP-independent manner.

GW182 recruits CCR4–NOT using a WG motif

Having shown that the CCR4–NOT complex associates with GW182 independently of PABP, we wished to identify the sequences within the silencing domain that are responsible for the interaction. A silencing domain fragment lacking the C-terminal domain (SD-3) bound PABP and the PAN2 deadenylase but failed to interact with the CCR4–NOT complex (**Fig. 1d**, compare lane 5 to 3). By contrast, a fragment lacking the Mid domain (SD-4) efficiently bound the CCR4–NOT complex but failed to interact with PABP and the majority of the PAN2 deadenylase (**Fig. 1d**, compare lane 6 to 3). These results bolster the conclusion that GW182 recruits the CCR4–NOT complex in a PABP-independent manner. In addition, these data demonstrate that the CCR4–NOT complex is recruited to GW182 through sequences in its C-terminal domain.

A more refined collection of deletions was generated to map the region in the C-terminal domain that mediates deadenylation and recruits the CCR4–NOT complex (**Fig. 2a**). Removing up to 25 amino acids from the C terminus did not prevent deadenylation (SD-6 and SD-7 (**Fig. 2b**)). In sharp contrast to this, deleting an additional 30 or 45 amino acids (SD-8 and SD-9, respectively) abrogated deadenylation (**Fig. 2b**).

A sequence alignment of GW182 C-terminal domains from different species revealed a stretch of conserved residues within the 31 amino acids (1635–1665) that is required for deadenylation. This stretch contained a leucine-tryptophan-glycine (LWG) triplet repeat (**Fig. 2a** and **Supplementary Fig. 2**). Alignment of *Drosophila melanogaster* GW182 (or other dipteran GW182 proteins) with mammalian GW182 proteins failed to reveal any LWG conserved residues (data not shown). However, two other insects (Pea aphid (*Acyrthosiphon pisum* (Ap) Gawky) and the European honey bee (*Apis mellifera* (Am) Gawky)) contained this conserved sequence in their GW182 C termini (**Supplementary Fig. 2**). The role of the LWG repeats in miRNA-mediated deadenylation was investigated by mutating them individually (SD-MUT1 and SD-MUT2) or together (SD-MUT3) to alanines (L1647A W1648A G1649A and/or L1658A W1659A G1660A; **Fig. 2a**,**b**). Mutating all of the amino acids in each LWG triplet to alanines (SD-MUT1 and SD-MUT2) had moderate effects on deadenylation (~50% deadenylation over 1 h (**Fig. 2b**)). However, mutating both LWG triplets to alanines (SD-MUT3) markedly impaired GW182-mediated deadenylation, which was not detected after 1 h. Furthermore, SD-MUT3 bound PABP as efficiently as SD-1 but associated only weakly with the CCR4–NOT deadenylase complex (**Fig. 2c**). These findings demonstrate that GW182 interacts with the CCR4–NOT deadenylase complex through a repeated LWG motif in its C-terminal domain to deadenylate target RNAs.

CNOT1 links CCR4–NOT to GW182 silencing domain

The CCR4–NOT deadenylase machinery is a large (~1.2 MDa) protein complex consisting of at least seven subunits[30]. We used a 'subtractive' pulldown approach to determine which CCR4–NOT complex subunit links GW182 to the deadenylation machinery. It was anticipated that the silencing domain would not associate with the CCR4–NOT complex if the GW182-interacting subunit were depleted. Conversely, we expected that depleting subunits that do not directly bind the silencing domain would not affect GW182 interaction with the remainder of the CCR4–NOT complex. Individual CCR4–NOT complex subunits (CNOT1, 6L and 7) were depleted from HeLa cells through shRNAi (**Fig. 3a**), and cytoplasmic extracts were incubated with a GST-tagged GW182 silencing domain fragment.

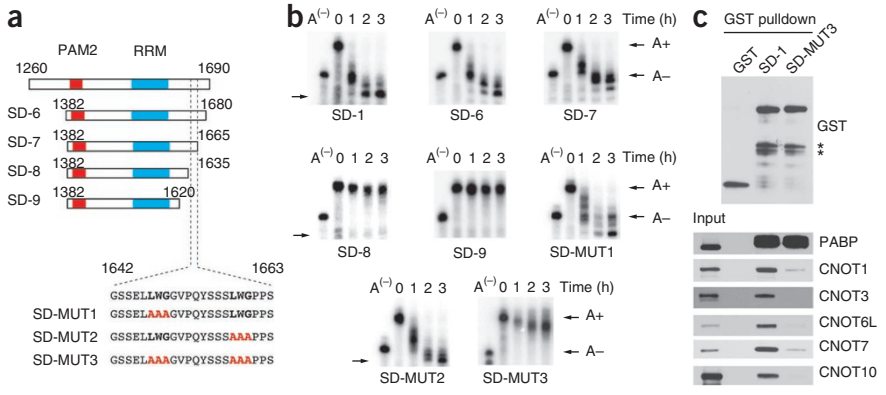

Figure 2 CCR4–NOT deadenylation complex interacts with an LWG repeat in GW182 C-terminal domain. (**a**) Schematic representation of human GW182 silencing domain fragments used in GST pulldown and deadenylation assays (**b**,**c**, respectively). Coordinates of deletions are marked to the left of each fragment. Dotted lines indicate the region required for efficient recruitment of the CCR4–NOT complex (**c**) and for promoting deadenylation (**b**). Mutations introduced in the context of SD-1 (SD-MUT1, MUT2 and MUT3) are also shown. (**b**) 5-BoxB-pA RNA deadenylation in the Krebs extract in the presence of GST-λN-HA-tagged TNRC6C silencing domain fragments outlined in **a**. SD-1-mediated deadenylation shown in **Figure 1c** is shown again in **b**. $A^{(-)}$ RNA was prepared as in **Figure 1**. RNAs shortened beyond the poly(A) tail are marked with an arrow on the left of the figure. Polyadenylated and deadenylated mRNAs are marked on the right of the figure. (**c**) Results from recombinant GST-λN-HA-tagged TNRC6C fragments (outlined in **a**) that were immobilized on glutathione-Sepharose beads and incubated with RNase A–treated HeLa cell lysates. Precipitated proteins were separated by SDS-PAGE and probed with antibodies against the indicated proteins. Partially degraded GST-tagged proteins are marked with asterisks on the right of the figure.

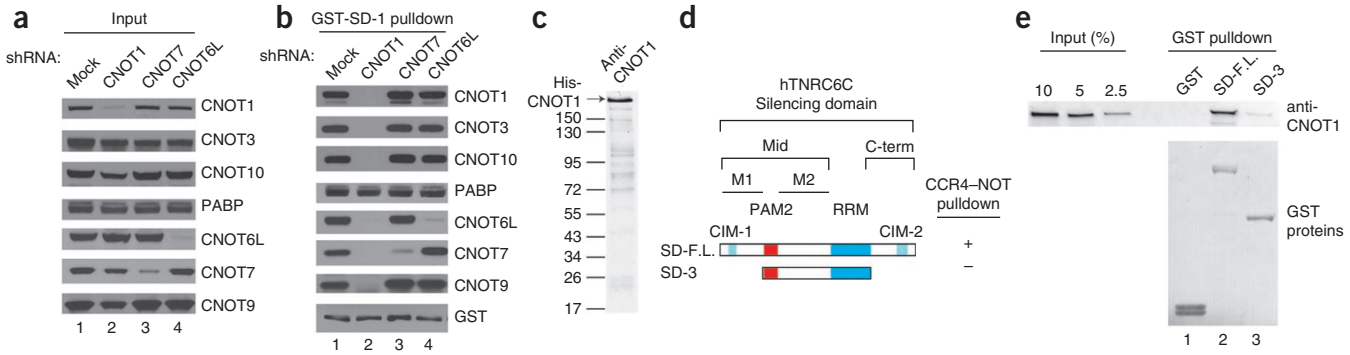

Figure 3 CNOT1 subunit links GW182 to the CCR4–NOT complex. (**a**) Western blotting of HeLa cell extracts depleted of CNOT1, CNOT6L or CNOT7 by shRNA and probed with antibodies against the indicated proteins. (**b**) Recombinant GST-λN-HA-tagged TNRC6C silencing domain fragment (SD-1) that was immobilized on glutathione-Sepharose beads and incubated with RNase A–treated shRNAi-depleted HeLa cell extracts. Precipitated proteins were resolved by SDS-PAGE and probed with antibodies against the indicated proteins. (**c**) Western blotting of recombinant His-tagged CNOT1 protein produced in SF9 insect cells with CNOT1 antibody. (**d**) Schematic representation of human GW182 silencing domain fragments used in GST pulldown assays (**e**). CCR4–NOT interaction motifs (CIMs) are depicted in light blue (see **Fig. 4** for more details). (**e**) Recombinant GST-λN-HA-tagged TNRC6C silencing domain fragments (**d**) were immobilized on glutathione-Sepharose beads and incubated with RNase A–treated recombinant CNOT1 protein. Proteins were separated by SDS-PAGE and probed with antibodies against the indicated proteins.

Fragment SD-1 failed to interact with any of the tested CCR4–NOT subunits from CNOT1-depleted cells (**Fig. 3b**, lane 2 compared to 1) even though all tested subunits were stable in CNOT1-depleted lysates (**Fig. 3a**, lane 2 compared to 1). Despite this, SD-1 did associate with both PABP and the PAN2 deadenylase in the absence of CNOT1 (**Fig. 3b** and **Supplementary Fig. 3**). Depleting CNOT7 or CNOT6L did not interfere with the interaction of SD-1 with the other subunits of the CCR4–NOT complex (**Fig. 3b**, lanes 3 and 4 compared to lane 1, respectively). Notably, several protein-protein interactions within the CCR4–NOT complex were stable despite the loss of the CNOT1. CNOT6L co-precipitated CNOT7, and CNOT3 co-precipitated CNOT2 equally well from CNOT1-depleted and mock-depleted lysates (**Supplementary Fig. 4a**,**b**). To test for a direct interaction between GW182 and CNOT1, we carried out GST pulldown experiments using recombinant GST-tagged GW182 silencing domain (SD-F.L.) and full-length His-tagged human (h)CNOT1 produced in insect SF9 cells (**Fig. 3c**–**e**). GST on its own did not interact with recombinant hCNOT1 (**Fig. 3e**, lane 1). However, GST-SD-F.L. bound CNOT1 (lane 2). By contrast, a GST-tagged silencing domain fragment lacking both CCR4–NOT interaction motifs (SD-3; see next section for details) failed to interact with CNOT1 (lane 3). Mass spectrometry analysis of GST pulldown reactions confirmed that SD-F.L. binds hCNOT1 without interacting with endogenous insect deadenylation machinery proteins (that is, CCR4–NOT subunits or PAN2/3) (**Supplementary Table 1**), thus excluding the possibility that the interaction between CNOT1 and GW182 is indirect. Taken together, these data show that GW182 directly binds CNOT1 to recruit the CCR4–NOT deadenylase complex.

Mid domain contains additional CCR4–NOT interacting motifs

To investigate whether regions that are N-terminal to the PAM2 motif might also contribute to CCR4–NOT recruitment, we extended the N terminus of the defective SD-9 fragment (**Fig. 4a**). Extending the N terminus of this fragment to include the M1 region rescued its interaction with the CCR4–NOT complex (SD-10; **Fig. 4a**,**b**, lane 3). The M1 region contains a highly evolutionarily conserved (from flies to humans) stretch of amino acids (TNRC6C coordinates ^{1294}QSRLXQW^{1300}) that could constitute an additional CCR4–NOT interacting motif (**Supplementary Fig. 5**). To investigate this possibility, several deletions and mutations were constructed (**Fig. 4a**). A truncated fragment (SD-11) that contained the conserved stretch of amino acids interacted with the CCR4–NOT complex (**Fig. 4b**, compare lane 6 to 3). By contrast, the CCR4–NOT complex failed to interact with fragments in which the motif was deleted (SD-12 through SD-14; **Fig. 4b**, compare lanes 7 through 9 to lane 3, respectively). Moreover, SD-10 failed to associate with the CCR4–NOT complex when six amino acids in the conserved stretch (QSRLXQW; **Supplementary Fig. 4**) were mutated to alanines (SD-MUT4; **Fig. 4b**, lane 4, compared to lane 3). Mutating a randomly chosen stretch of five residues within the M1 region to alanines (SD-MUT5) had no effect on CCR4–NOT complex binding (**Fig. 4b**, compare lane 5 to 3; **Supplementary Fig. 4**). To determine whether the CNOT1 subunit links the M1 region with the CCR4–NOT complex, we did GST pulldowns from mock-depleted and CNOT1-depleted extracts using the SD-10 fragment as bait. SD-10 did not associate with CNOT2, CNOT3, CNOT7, CNOT9 or CNOT10 from a CNOT1-depleted extract, whereas PABP and PAN2 interactions were unaffected (**Fig. 4c**, compare lane 4 to 3). Thus, the human GW182 silencing domain interacts with the CCR4–NOT complex through two distinct sequences that we call CCR4-interacting motifs (CIMs). CIM-1 resides within the M1 region of the Mid domain, whereas the C-terminal domain contains CIM-2 (LWG motif). Moreover, both CIMs interact with the CCR4–NOT complex through the CNOT1 subunit.

GW182 CIMs have distinct roles in deadenylation

Why does GW182 contact the CCR4–NOT complex through two independent sites? One possible advantage is that the two motifs act cooperatively to bind the deadenylation machinery, either additively or synergistically. To explore this possibility, we did GST pulldowns comparing GW182 fragments containing CIM-1 (SD-10), CIM-2 (SD-1) or both (SD-F.L.) (**Fig. 4d**). All three fragments interacted with the PAN2 deadenylase to similar extents (**Fig. 4d**, compare lanes 1–3 (SD-F.L.) with lanes 4–6 (SD-10) and lanes 7–9 (SD-1)). Unexpectedly, ~16-fold more CNOT3, CNOT7 and CNOT9 protein was bound to a GW182 fragment containing both CIMs (SD-F.L.) than was bound by a fragment containing only CIM-2 (SD-1) (lanes 7–9 compared to lanes 1–3). Also, ~10-fold more of CNOT3, CNOT7 and CNOT9 subunits associated with a GW182 fragment containing only CIM-1 (SD-10).

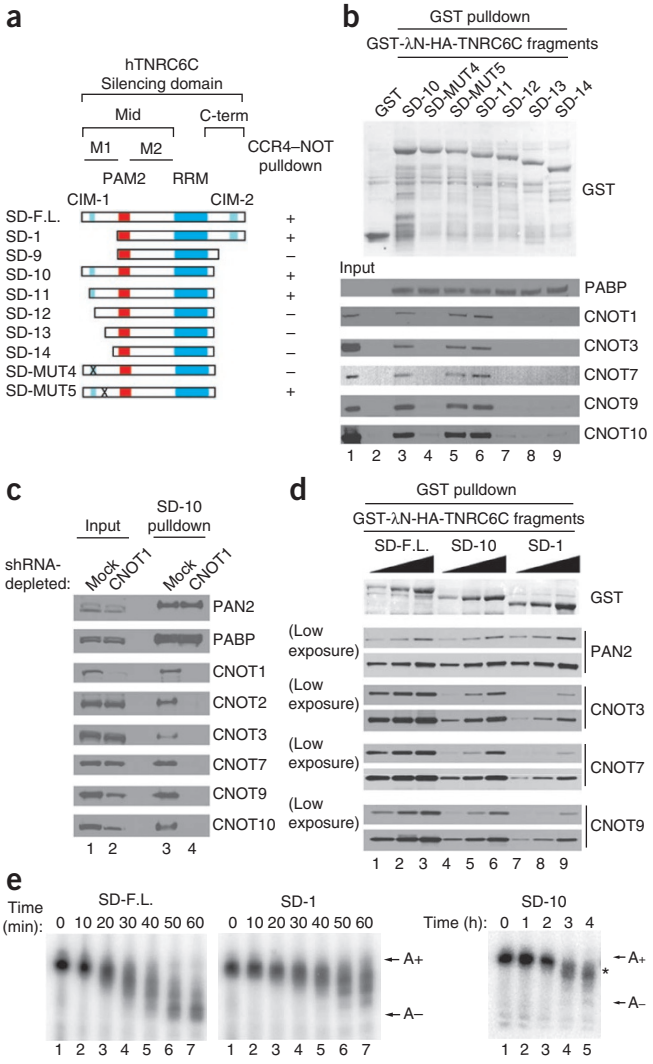

Figure 4 The GW182 middle domain contains a second CCR4–NOT binding site. (**a**) Schematic representation of human GW182 silencing domain fragments used in GST pulldown and deadenylation assays (**b**–**e**, respectively). CCR4–NOT interaction motifs (CIMs) are depicted in light blue. Coordinates of deletions are marked to the left of each fragment. M1 region point mutations, denoted by 'X', are described in **Supplementary Figure 4**. (**b**) Recombinant GST-λN-HA-tagged TNRC6C-silencing domain fragments were immobilized on glutathione-Sepharose beads and incubated with RNase A–treated HeLa cell extracts. Proteins were separated by SDS-PAGE and probed with antibodies against the indicated proteins. (**c**) Recombinant GST-λN-HA-tagged SD-10 was immobilized on glutathione-Sepharose beads and incubated with RNase A–treated shRNAi-depleted HeLa cell extracts. Precipitated proteins were separated by SDS-PAGE and probed with antibodies against the indicated proteins. (**d**) Increasing concentrations of recombinant GST-λN-HA-tagged TNRC6C fragments (SD-F.L., SD-10 and SD-1) were immobilized on glutathione-Sepharose beads and incubated with RNase A–treated HeLa cell extracts. Precipitated proteins were separated by SDS-PAGE and probed with antibodies against the indicated proteins. (**e**) 5-BoxB-pA RNA deadenylation in the Krebs extract that deadenylates at a slightly slower rate in the presence of GST-λN-HA-tagged TNRC6C fragments SD-F.L., SD-1 and SD-10 as compared to **Figures 1** and **2**. Polyadenylated and deadenylated mRNAs are marked on the right of the figure. The faster migrating RNA species for SD-10 is marked with an asterisk.

Next, we wished to correlate the binding of GW182 fragments to CNOT1 with deadenylation in Krebs extract. A full-length silencing domain (SD-F.L.) containing both CIMs initiated deadenylation faster (~50% deadenylation within 30 min compared to 50 min) than a fragment containing only CIM-2 (SD-1) (**Fig. 4e**). However, a fragment containing only CIM-1 (SD-10) could not engender complete deadenylation. Tethering SD-10 initiated deadenylation, with approximately 15 As removed by 3 and 4 h after incubation (marked by an asterisk). However, deadenylation stalled and did not progress any further. It is conceivable that this stalling was caused by SD-10 being defective in assisting the displacement of PABP from the poly(A) tail (see Discussion). These results suggest that the GW182 CIM-1 and CIM-2 possess distinct but complementary roles in miRNA silencing. CIM-1 assists CIM-2 to bind the CCR4–NOT complex and initiate deadenylation but cannot bring about complete poly(A) shortening on its own. Notably, these results indicate that GW182 has two independent functions in miRNA-mediated deadenylation. One function is to recruit the CCR4–NOT complex to target RNAs and the second is to act as a deadenylation coactivator that assists the CCR4–NOT complex to degrade the poly(A) tail.

DISCUSSION

Two motifs in GW182 recruit CCR4–NOT

We show here that GW182 effects deadenylation of target RNAs by interacting with the CCR4–NOT deadenylase complex through two distinct and separate sequences. The two GW182-CCR4–NOT interaction motifs (CIMs) are at the opposite ends of the GW182 silencing domain, one in the M1 region of the middle domain (CIM-1) and the other in the C-terminal domain (CIM-2) (**Figs. 4a** and **5**). We demonstrate that the CCR4–NOT complex is recruited by GW182 to the RISC in a PABP-independent manner. Mutating or deleting the GW182 PAM2 motif abrogated PABP binding but did not affect GW182 interaction with the CCR4–NOT complex (**Fig. 1**). Moreover, our data show that both CIMs interact with the CCR4–NOT complex through CNOT1, a component of the deadenylase complex that serves as a scaffold for other subunits (**Figs. 3** and **4**).

CIM-1 is conserved between insects (including dipterans) and mammals, (**Supplementary Fig. 5**). By contrast, CIM-2 is found in mammals but only in certain insects (honey bees and aphids) and not in dipterans (**Supplementary Fig. 2**). Unlike human GW182 that directly binds PABP through its PAM2 motif, *Drosophila melanogaster* GW182 preferentially interacts with PABP through its C-terminal domain[20,21]. Thus, *D. melanogaster* GW182 may utilize CIM-1 alone or in combination with other sequences to interact with the deadenylase machinery on miRNA-targeted mRNAs.

GW182 proteins are named after the array of glycine-tryptophan repeats (either GW, WG or GWG)[16] in the N-terminal domain that bind to AGO and thus recruit GW182 to the RISC. Mammalian GW182 proteins contain additional glycine-tryptophan repeats in the middle and C-terminal domains that do not bind AGO. Whether these additional repeats have important roles in miRNA silencing has not been known until now[16]. We provide evidence here that a glycine-tryptophan repeat in the GW182 C-terminal domain (CIM-2) forms a genuine docking site for the CCR4–NOT complex. Thus, GW182 proteins interact with both AGO proteins and the CCR4–NOT complex through glycine-tryptophan repeats in their N- and C-terminal domains, respectively.

GW182–PABP associates with PAN deadenylase machinery

The CCR4–NOT complex is integral to miRNA-mediated deadenylation, whereas the PAN complex, comprised of the PAN2 deadenylase and PAN3, is dispensable[5,31,32]. We show that GW182 also associates with the PAN2 deadenylase. In contrast to the CCR4–NOT complex,

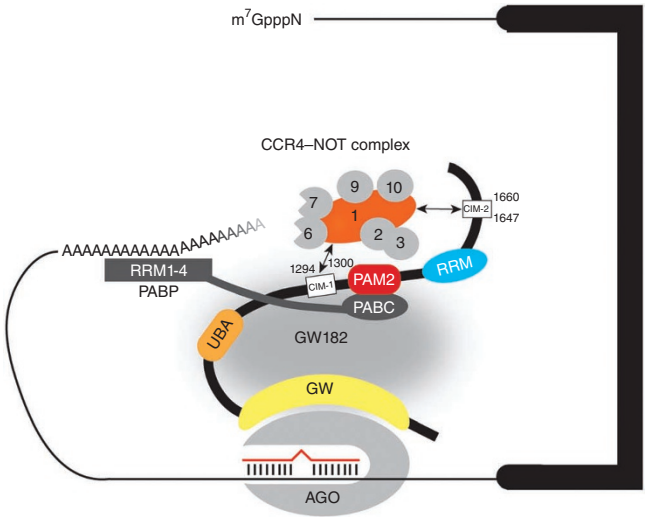

Figure 5 Model for GW182 coordinating miRNA-mediated deadenylation. GW182 binds Argonaute (AGO) through its N-terminal GW-rich domain to form the miRISC. GW182 recruits the poly(A) tail into the vicinity of the miRISC by interacting with PABP through the PAM2/PABC contact. Two CCR4–NOT interaction motifs (CIMs) in the GW182 recruit the CCR4–NOT complex to facilitate deadenylation of miRNA-targeted mRNAs. CIM-1 and CIM-2 are labeled with their coordinates in the human GW182 paralog TNRC6C. The CNOT1 subunit interaction with GW182 is depicted with two-sided arrows. The PAN2–PAN3 interaction with PABP has been purposely excluded to simplify the figure.

which interacts with GW182 in a PABP-independent manner, the PAN2 deadenylase associates with the GW182 PAM2 motif, most likely through PABP (**Fig. 1d**). PABP interacts with the PAN2 deadenylase through the PAN3 bridging protein[27–29]. Thus, our results are consistent with the GW182–PABP complex also using PAN3 to associate with the PAN2 deadenylase. It has recently been hypothesized that the PAN2–PAN3 and CCR4–NOT deadenylase complexes might assemble to form a 'supercomplex' *in vivo*[33]; however, our data suggest that GW182 interacts with the CCR4–NOT complex in a PAN complex–independent manner and vice versa (**Figs. 1d**, **4c** and **Supplementary Fig. 3**). Thus, our data are consistent with the model that GW182 facilitates miRNA-mediated deadenylation by interacting with the PAN and CCR4–NOT deadenylase machineries through separate motifs and as independent complexes. Whether both deadenylase complexes are bound by GW182 at the same time or sequentially remains to be established.

GW182 is a deadenylase coactivator

Individually, each GW182-CCR4–NOT interaction motif (CIM-1 or CIM-2) binds the CCR4–NOT complex; however, these motifs are not functionally redundant. A GW182 silencing domain fragment containing only CIM-2 (SD-1) deadenylates the mRNA. In marked contrast to this, a GW182 silencing fragment containing only CIM-1 (SD-10) initiates, but does not support, processive deadenylation, as evidenced by the presence of a slightly faster migrating RNA species during *in vitro* deadenylation reactions (**Fig. 4e**). Thus, GW182 has at least two roles in miRNA-mediated deadenylation. Firstly, GW182 serves as a binding platform that recruits two deadenylase complexes to target RNAs. Secondly, GW182 acts as a deadenylation coactivator by assisting the CCR4–NOT complex to shorten the poly(A) tail.

How does GW182 assist the CCR4–NOT complex in the deadenylation reaction? PABP binds GW182 and is an essential coactivator for initiating miRNA-mediated deadenylation[15,23]. However, PABP must be displaced from the poly(A) tail before it can be deadenylated[34,35]. Indeed, a GW182 silencing domain fragment that cannot bind PABP (SD-4) failed to show processive deadenylation. Namely, the deadenylase stalled along the 98-nt poly(A) tail at increments of approximately 27 As, which is the number of adenosines bound by a single PABP (**Fig. 1c**, marked with asterisks)[36]. GW182 may therefore act in concert with the CCR4–NOT complex to displace PABP from the poly(A) tail, allowing processive deadenylation.

In conclusion, we report here that GW182 independently tethers two deadenylase machineries by means of independent motifs and has a newly identified role as a deadenylase coactivator in the processive deadenylation of mRNA targets. Our studies and those of others demonstrate that the GW182 silencing domain brings about translational repression and deadenylation of target RNAs. It remains to be determined whether AGO binding induces conformational changes in GW182 that influence recruitment of the deadenylation machineries. Moreover, although the CCR4–NOT complex can contact GW182 through CIM-1 and CIM-2, it will be interesting to determine whether both CIMs are required for every mRNA target *in vivo* and in every cell type. The mRNA translation state, 3′ UTR secondary structure and differences between GW182 paralogs and isoforms may all modulate the context of CIM1 and CIM2 contributions. Insight into the regulation of the various GW182 interactions and activities should yield answers to prevailing conundrums on apparent mechanistic differences in miRNA action between cells, tissues and organisms.

Note added in proof: Results presented here are consistent with two other publications[37,38] *describing interactions between GW182 and the CCR4–NOT complex.*

METHODS

Methods and any associated references are available in the online version of the paper at http://www.nature.com/nsmb/.

Note: Supplementary information is available on the Nature Structural & Molecular Biology website.

ACKNOWLEDGMENTS

We thank G. Hannon (Cold Spring Harbor Laboratory) for providing rabbit polyclonal CNOT10 antibody; A.-B. Shyu (University of Texas Medical School) for rabbit polyclonal PAN2 antibody; W. Filipowicz (Friedrich Miescher Institute for Biomedical Research) for TNRC6C and LacZ plasmids; and M. Jinek, T. Sundermeier and I. Topisirovic for helpful discussions. This work was supported by a Canadian Institutes of Health Research (CIHR) grant to N.S.

AUTHOR CONTRIBUTIONS

M.R.F., T.F.D. and N.S. designed experiments. M.R.F., M.K.C., J.G. and M.M. conducted experiments. T.S. and B.R. conducted mass spectrometry analysis. F.F. and B.N. purified recombinant CNOT1 protein. T.Y. provided CNOT antibodies. M.R.F., T.F.D. and N.S. wrote the manuscript.

COMPETING FINANCIAL INTERESTS

The authors declare no competing financial interests.

Published online at http://www.nature.com/nsmb/.
Reprints and permissions information is available online at http://www.nature.com/reprints/index.html.

1. Filipowicz, W., Bhattacharyya, S.N. & Sonenberg, N. Mechanisms of post-transcriptional regulation by microRNAs: are the answers in sight? *Nat. Rev. Genet.* **9**, 102–114 (2008).
2. Huntzinger, E. & Izaurralde, E. Gene silencing by microRNAs: contributions of translational repression and mRNA decay. *Nat. Rev. Genet.* **12**, 99–110 (2011).
3. Fabian, M.R., Sonenberg, N. & Filipowicz, W. Regulation of mRNA translation and stability by microRNAs. *Annu. Rev. Biochem.* **79**, 351–379 (2010).

4. Rehwinkel, J., Behm-Ansmant, I., Gatfield, D. & Izaurralde, E. A crucial role for GW182 and the DCP1:DCP2 decapping complex in miRNA-mediated gene silencing. *RNA* **11**, 1640–1647 (2005).
5. Behm-Ansmant, I. *et al.* mRNA degradation by miRNAs and GW182 requires both CCR4:NOT deadenylase and DCP1:DCP2 decapping complexes. *Genes Dev.* **20**, 1885–1898 (2006).
6. Eulalio, A., Huntzinger, E. & Izaurralde, E. GW182 interaction with Argonaute is essential for miRNA-mediated translational repression and mRNA decay. *Nat. Struct. Mol. Biol.* **15**, 346–353 (2008).
7. Jakymiw, A. *et al.* The role of GW/P-bodies in RNA processing and silencing. *J. Cell Sci.* **120**, 1317–1323 (2007).
8. Liu, J. *et al.* A role for the P-body component GW182 in microRNA function. *Nat. Cell Biol.* **7**, 1261–1266 (2005).
9. Meister, G. *et al.* Identification of novel argonaute-associated proteins. *Curr. Biol.* **15**, 2149–2155 (2005).
10. Zipprich, J.T., Bhattacharyya, S., Mathys, H. & Filipowicz, W. Importance of the C-terminal domain of the human GW182 protein TNRC6C for translational repression. *RNA* **15**, 781–793 (2009).
11. Chekulaeva, M., Parker, R. & Filipowicz, W. The GW/WG repeats of *Drosophila* GW182 function as effector motifs for miRNA-mediated repression. *Nucleic Acids Res.* **38**, 6673–6683 (2010).
12. Eulalio, A., Helms, S., Fritzsch, C., Fauser, M. & Izaurralde, E. A C-terminal silencing domain in GW182 is essential for miRNA function. *RNA* **15**, 1067–1077 (2009).
13. Lazzaretti, D., Tournier, I. & Izaurralde, E. The C-terminal domains of human TNRC6A, TNRC6B, and TNRC6C silence bound transcripts independently of Argonaute proteins. *RNA* **15**, 1059–1066 (2009).
14. Baillat, D. & Shiekhattar, R. Functional dissection of the human TNRC6 (GW182-related) family of proteins. *Mol. Cell Biol.* **29**, 4144–4155 (2009).
15. Jinek, M., Fabian, M.R., Coyle, S.M., Sonenberg, N. & Doudna, J.A. Structural insights into the human GW182-PABC interaction in microRNA-mediated deadenylation. *Nat. Struct. Mol. Biol.* **17**, 238–240 (2010).
16. Eulalio, A., Tritschler, F. & Izaurralde, E. The GW182 protein family in animal cells: new insights into domains required for miRNA-mediated gene silencing. *RNA* **15**, 1433–1442 (2009).
17. Takimoto, K., Wakiyama, M. & Yokoyama, S. Mammalian GW182 contains multiple Argonaute-binding sites and functions in microRNA-mediated translational repression. *RNA* **15**, 1078–1089 (2009).
18. Lian, S.L. *et al.* The C-terminal half of human Ago2 binds to multiple GW-rich regions of GW182 and requires GW182 to mediate silencing. *RNA* **15**, 804–813 (2009).
19. Eulalio, A. *et al.* The RRM domain in GW182 proteins contributes to miRNA-mediated gene silencing. *Nucleic Acids Res.* **37**, 2974–2983 (2009).
20. Huntzinger, E., Braun, J.E., Heimstadt, S., Zekri, L. & Izaurralde, E. Two PABPC1-binding sites in GW182 proteins promote miRNA-mediated gene silencing. *EMBO J.* **29**, 4146–4160 (2010).
21. Zekri, L., Huntzinger, E., Heimstadt, S. & Izaurralde, E. The silencing domain of GW182 interacts with PABPC1 to promote translational repression and degradation of microRNA targets and is required for target release. *Mol. Cell Biol.* **29**, 6220–6231 (2009).
22. Kozlov, G., Safaee, N., Rosenauer, A. & Gehring, K. Structural basis of binding of P-body-associated proteins GW182 and ataxin-2 by the MIle domain of poly(A)-binding protein. *J. Biol. Chem.* **285**, 13599–13606 (2010).
23. Fabian, M.R. *et al.* Mammalian miRNA RISC recruits CAF1 and PABP to affect PABP-dependent deadenylation. *Mol. Cell* **35**, 868–880 (2009).
24. Goldstrohm, A.C. & Wickens, M. Multifunctional deadenylase complexes diversify mRNA control. *Nat. Rev. Mol. Cell Biol.* **9**, 337–344 (2008).
25. Mathonnet, G. *et al.* MicroRNA inhibition of translation initiation *in vitro* by targeting the cap-binding complex eIF4F. *Science* **317**, 1764–1767 (2007).
26. Wu, E. *et al.* Pervasive and cooperative deadenylation of 3′UTRs by embryonic microRNA families. *Mol. Cell* **40**, 558–570 (2010).
27. Siddiqui, N. *et al.* Poly(A) nuclease interacts with the C-terminal domain of polyadenylate-binding protein domain from poly(A)-binding protein. *J. Biol. Chem.* **282**, 25067–25075 (2007).
28. Uchida, N., Hoshino, S. & Katada, T. Identification of a human cytoplasmic poly(A) nuclease complex stimulated by poly(A)-binding protein. *J. Biol. Chem.* **279**, 1383–1391 (2004).
29. Brown, C.E., Tarun, S.Z. Jr., Boeck, R. & Sachs, A.B. PAN3 encodes a subunit of the Pab1p-dependent poly(A) nuclease in *Saccharomyces cerevisiae*. *Mol. Cell Biol.* **16**, 5744–5753 (1996).
30. Lau, N.C. *et al.* Human Ccr4-Not complexes contain variable deadenylase subunits. *Biochem. J.* **422**, 443–453 (2009).
31. Piao, X., Zhang, X., Wu, L. & Belasco, J.G. CCR4-NOT deadenylates mRNA associated with RNA-induced silencing complexes in human cells. *Mol. Cell Biol.* **30**, 1486–1494 (2010).
32. Chen, C.Y., Zheng, D., Xia, Z. & Shyu, A.B. Ago-TNRC6 triggers microRNA-mediated decay by promoting two deadenylation steps. *Nat. Struct. Mol. Biol.* **16**, 1160–1166 (2009).
33. Zheng, D. *et al.* Deadenylation is prerequisite for P-body formation and mRNA decay in mammalian cells. *J. Cell Biol.* **182**, 89–101 (2008).
34. Simón, E. & Seraphin, B. A specific role for the C-terminal region of the Poly(A)-binding protein in mRNA decay. *Nucleic Acids Res.* **35**, 6017–6028 (2007).
35. Tucker, M., Staples, R.R., Valencia-Sanchez, M.A., Muhlrad, D. & Parker, R. Ccr4p is the catalytic subunit of a Ccr4p/Pop2p/Notp mRNA deadenylase complex in *Saccharomyces cerevisiae*. *EMBO J.* **21**, 1427–1436 (2002).
36. Baer, B.W. & Kornberg, R.D. Repeating structure of cytoplasmic poly(A)-ribonucleoprotein. *Nat. Struct. Mol. Biol* **77**, 1890–1892 (1980).
37. Chekulaeva, M. *et al.* miRNA repression involves GW182-mediated recruitment of CCR4–NOT through conserved W-containing motifs. *Nat. Struct. Mol. Biol.* doi:10.1038/nsmb.2166 (published online 7 Oct 2011).
38. Braun, J.E., Huntzinger, E., Fauser, M. & Izaurralde, E. GW182 proteins directly recruit cytoplasmic deadenylase complexes to miRNA targets. *Mol. Cell* **43**, doi:10.1016/j.molcel.2011.09.007 (2011).

ONLINE METHODS

DNA constructs and transfections of HeLa cells. For preparation of recombinant proteins, human TNRC6C fragments were PCR amplified and subcloned into pGEX-6p1 (GE Healthcare) in frame with an upstream sequence encoding a λN-HA peptide and a C-terminal Flag epitope. Purification of recombinant TNRC6C fragments was previously described[39]. For expression in HeLa cells, full-length human TNRC6C and its fragments were PCR amplified and subcloned into pcDNA3.1 (Invitrogen) in frame with an upstream sequence encoding an HA epitope or a λN-HA peptide. A pCI-neo (Promega) vector encoding λN-HA-LacZ, generously provided by W. Filipowicz, was used as a negative control.

Antibodies. Antibodies against CNOT1, CNOT2, CNOT3, CNOT6L, CNOT7 and CNOT9 were previously described[40–42]. CNOT10 and PAN2 antibodies were kind gifts from G. Hannon and A.-B. Shyu, respectively. Mouse monoclonal anti-HA and anti-β-actin were from Covance and Sigma, respectively. Rabbit polyclonal anti-HA was from Sigma.

Glutathione-*S*-transferase pulldown and co-immunoprecipitation experiments. HeLa cells were collected, washed twice with PBS buffer, pelleted and flash frozen in liquid nitrogen. Pellets were resuspended in assay buffer 25 mM HEPES-KOH, pH 7.3, 300 mM KCl, 75 mM KOAc, 2 mM $MgCl_2$, 0.5% (v/v) NP-40 and supplemented with protease inhibitors (Roche). Lysates were clarified by centrifuging once at 20,000*g* for 30 min. HeLa cell lysates were precleared with glutathione Sepharose-4B (GE Life Sciences) or protein G-agarose (Millipore) for 1 h at 4 °C with gentle rocking. For immunopreciptation experiments, 1 ml of precleared lysates (2 mg ml^{-1}) was incubated with RNase A (Sigma), 20 µl of packed protein G-agarose and 1 µg of mouse monoclonal or polyclonal HA, anti-CNOT6L or anti-CNOT3 antibody at 4 °C for 5 h with gentle rocking. For GST pulldown experiments, 1 ml of pre-cleared lysate (2 mg ml^{-1}) was incubated with 10 µg of RNase A (Sigma), 20 µl of packed glutathione Sepharose-4B and 100 pmol of GST, or various recombinant GST-λN-HA-TNRC6C fragments for 5 h at 4 °C with gentle rocking. In both experiments, beads were washed five times with 1 ml of assay buffer, and proteins were eluted by boiling the beads with 40 µl of Laemmli sample buffer at 95 °C for 8 min. Proteins were separated by SDS-PAGE followed by western blotting.

Recombinant protein expression and purification. GST-λN-HA-TNRC6C-Flag proteins were expressed in Rosetta-2(DE3) *Escherichia coli* cells (EMD Biosciences) and purified by two sequential affinity chromatography steps, first over glutathione Sepharose 4B resin (GE Life Sciences), followed by M2-Flag affinity resin (Sigma). His-tagged human CNOT1 was subcloned into pFastBac Htb (Invitrogen). SF9 cells were infected with CNOT1 encoding virus and cells were harvested 72 h after infection. His-CNOT1 expressing cells were lysed in 50 mM Tris-HCl (pH 8.0), 1M NaCl, 20 mM imidazole (pH 8.0) and 10% (v/v) glycerol. Clarified lysate was incubated with Ni-NTA resin (Qiagen), washed extensively with a lysis buffer and eluted in 50 mM Tris-HCl (pH 8.0), 1 M NaCl; 250 mM imidazole (pH 8.0) and 10% (v/v) glycerol.

Mass spectrometry analysis of GST pulldown complexes. Samples were treated with 4–12% SDS-PAGE (BioRad) and run ~5 cm into the gel. The entire contents of each lane were excised and proteolyzed with trypsin. Peptides were analyzed by means of nanoflow liquid chromatography–tandem mass spectrometry (nLC-MS/MS) and a hybrid linear quadrupole ion trap (Velos Orbitrap) mass spectrometer coupled to a Proxeon Easy-nLC pump flow system (ThermoFisher Scientific). Data were searched against *Spodoptera frugiperda*–expressed sequence tags (downloaded from http://bioweb.ensam.inra.fr/spodobase/) translated in all six reading frames, as well as against the *D. melanogaster* and silkworm (*Bombyx mori*) (curated and predicted) ORF sequences, using X!Tandem[43]. Two unique peptides with an expect score of <−2 were required for protein identifications.

***In vitro* deadenylation assays.** 5-BoxB-pA RNA transcripts were generated from a PCR product derived from RL-5-BoxB-pA. PCR product was digested with AgeI and blunted with mung bean nuclease (New England Biolabs). To synthesize radiolabeled mRNAs [α-^{32}P]UTP (800 Ci $mmol^{-1}$, 10 mCi ml^{-1}; PerkinElmer) was used according to the manufacturer's protocol. The mRNA was loaded on a mini Quick Spin RNA Column (Roche) to remove unincorporated nucleotides. *In vitro* deadenylation assays were carried out as previously described in the presence of 172 nM GST-λN-HA-TNRC6C-Flag protein fragments[39,44]. Recombinant proteins used in deadenylation assays were produced using previously described methods[39].

Depleting CNOT1, CNOT6L, CNOT7 and PAN3 by RNA interference. HeLa cells growing in 6-well plates were transduced with pLKO.1 lentiviruses that code for short hairpins targeting either human CNOT1 (5′-CATTCAACATTCCCTTATAAA-3′), CNOT6L (5′-CCCAGAGTATTCTGATGTGAA-3′), CNOT7 (5′-GCTGACTATCAATACCAACTA-3′) or a scrambled control sequence (5′-AACAAGATGAAGAGCACCAA-3′) (Sigma Aldrich). Puromycin (5 µg ml^{-1}) was added to the cell cultures 48 h after lentiviral transduction to select for cells with integrated lentivirus, and cell cultures were subsequently expanded. Cytoplasmic extracts were generated from cell cultures, and depletion of various deadenylation factors was verified by western blotting.

39. Jinek, M., Fabian, M.R., Coyle, S.M., Sonenberg, N. & Doudna, J.A. Structural insights into the human GW182-PABC interaction in microRNA-mediated deadenylation. *Nat. Struct. Mol. Biol.* **17**, 238–240 (2010).
40. Ito, K. *et al.* CNOT2 depletion disrupts and inhibits the CCR4-NOT deadenylase complex and induces apoptotic cell death. *Genes Cells* **16**, 368–379 (2011).
41. Miyasaka, T. *et al.* Interaction of antiproliferative protein Tob with the CCR4-NOT deadenylase complex. *Cancer Sci.* **99**, 755–761 (2008).
42. Morita, M. *et al.* Depletion of mammalian CCR4b deadenylase triggers elevation of the p27Kip1 mRNA level and impairs cell growth. *Mol. Cell Biol.* **27**, 4980–4990 (2007).
43. Craig, R., Cortens, J.P. & Beavis, R.C. Open source system for analyzing, validating, and storing protein identification data. *J. Proteome Res.* **3**, 1234–1242 (2004).
44. Fabian, M.R. *et al.* Mammalian miRNA RISC recruits CAF1 and PABP to affect PABP-dependent deadenylation. *Mol. Cell* **35**, 868–880 (2009).

doi:10.1038/nsmb.2149